Instruments and Methods

A dynamic method to measure the shear strength of snow

Tsutomu NAKAMURA,[1] Osamu ABE,[2] Ryuhei HASHIMOTO,[3] Takeshi OHTA[4]

[1]39-134 Okurayama, Kohata, Uji, Kyoto 611-0002, Japan
E-mail: ntom@arrow.ocn.ne.jp
[2]Snow and Ice Research Center, National Research Institute for Earth Science and Disaster Prevention (NIED), 1400 Tokamachi, Shinjo 996-0091, Japan
[3]Lost Arrow Inc. 1386-6, Suneori, Tsurugashima 350-2213, Japan
[4]Graduate School of Bioagricultural Sciences, Nagoya University, Nagoya 464-8601, Japan

ABSTRACT. A new vibration apparatus for measuring the shear strength of snow has been designed and fabricated. The force applied to a snow block is calculated using Newton's second law. Results from this apparatus concerning the dependence of the shear strength on snow density, overburden load and strain rate are in reasonable agreement with those obtained from the work of previous researchers. Snow densities ranged from 160 to 320 kg m^{-3}. The overburden load and strain rate ranged from 1.95×10^{-1} to 7.79×10^{-1} kPa and 2.9×10^{-4} to 9.1×10^{-3} s^{-1} respectively.

INTRODUCTION

Shear strength is one of the fundamental mechanical properties of snow. On a microphysical scale, the mechanical properties of snow are greatly dependent upon and relevant to the microstructure. For snow avalanche researchers, shear strength is a critical factor in determining whether avalanches will occur or not. Earthquakes occurring in the snow season can trigger snow avalanches as reported, for example, in Japan (Higashiura and others, 1979) and Turkey (Gürer, 1993). The shear strength is also of interest to those living in the heavy-snowfall areas of Japan because they need to consider when the snow that accumulates on sloping roofs will be released (e.g. Nakamura and others, 1992, 1997, 2000).

The shear strength of snow has been measured by many researchers with many different apparatuses and testers in both controlled laboratories and in situ field tests. For example, McClung (1977) and Schweizer (1998) used a direct simple shear apparatus in controlled laboratories.

In situ field tests involving the use of portable and handy shear frame testers have been performed by many researchers (e.g. Perla and others, 1982; Perla and Beck, 1983; Föhn, 1987; Jamieson and Johnston, 2001; Abe, 2004; Abe and others, 2006). Watanabe (1977) and Yamanoi and Endo (2002) used shear revolving testers, though the sample sizes considered in these studies were different. These studies have firmly established that snow shear strength is dependent on density. In addition, shear strength is dependent on overburden weight and strain rate. However, a large volume of data is yet to be obtained to study the overburden-weight and strain-rate dependencies. More data are required to establish these dependencies, and we believe our new instrument suffices to measure these data.

PRINCIPLE OF MEASURING SNOW SHEAR STRENGTH BY THE PROPOSED METHOD

When a snow block of mass m is frozen in a rectangular metal dish and is swiftly accelerated horizontally, an inertial force, F, expressed as (Newton's second law)

$$F = m\alpha, \tag{1}$$

is applied to the snow block, where α is the acceleration applied to the snow block. The acceleration can be measured using an accelerogram (Fig. 1).

If the shear strength of a snow block is less than the given inertial force, then the snow block will fracture. The critical strength is the shear strength, τ (kPa), of the snow block given as

$$\tau = F/A, \tag{2}$$

where F is the force (kN) applied to the snow block, and A is the fractured snow area (m^2).

APPARATUS

Our vibration apparatus for measuring the shear strength of snow is shown in Figure 2. It consists of a mechanical part and an electrical part. An electric motor is connected to a snow-loaded slider by a crankshaft. This slider is placed on two Z-shaped guide rails (Fig. 3) fixed on the metal base. The aluminium dish fixed to the slider, in which the snow sample is frozen, is 0.4 m long, 0.3 m wide and 0.015 m deep. The dish moves to and fro on the Z-shaped guide rails. The slider

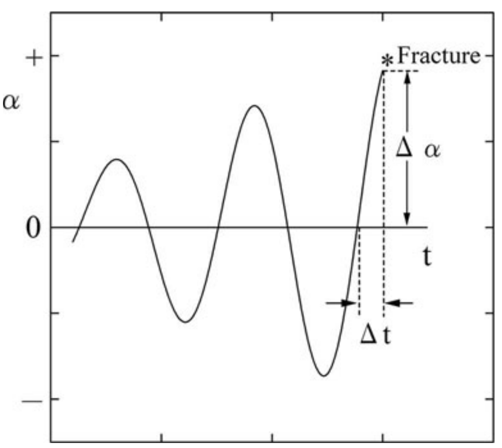

Fig. 1. Schematic representation of an accelerogram showing the fracture point.

https://doi.org/10.3189/002214310791968502 Published online by Cambridge University Press

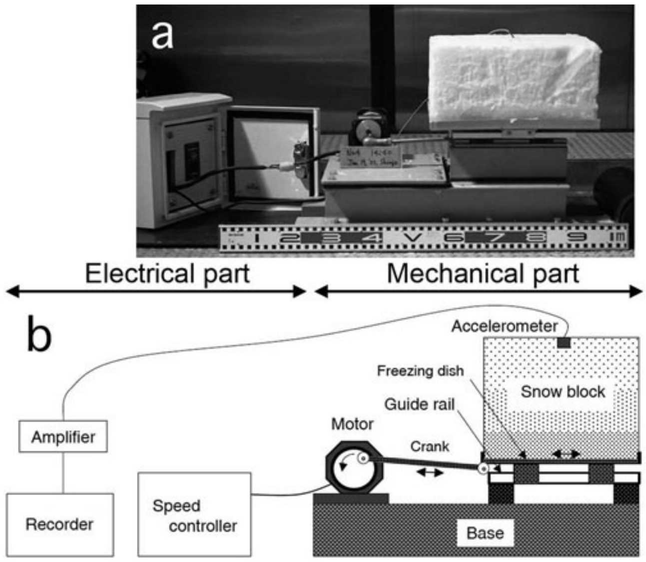

Fig. 2. Schematic representation and photograph of the apparatus.

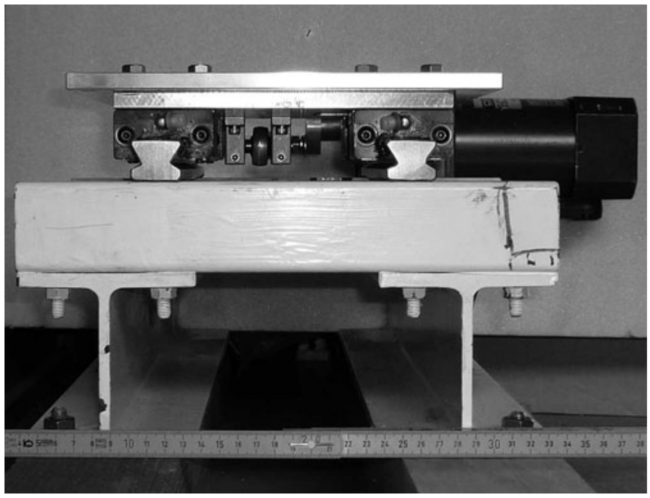

Fig. 3. Two Z-shaped guide rails fixed on a metal base, and a slider on which the aluminium dish is fixed.

vibrates as the motor rotates. The power of the electric motor is 90 W. The speed of the motor is regulated by a controller. The available acceleration ranges from 10 to 120 m s^{-2}. The accelerogram is recorded on a pen recorder through an amplifier (Fig. 4).

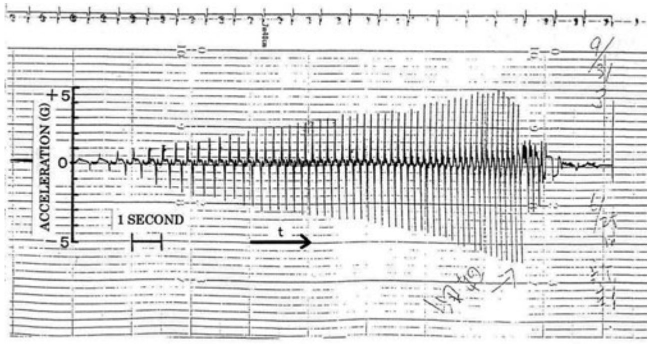

Fig. 4. An example of an accelerogram.

SNOW SAMPLES

Two groups of snow samples were tested: refrozen rounded polycrystals and small rounded particles (Colbeck and others, 1990, p. 1–23 and table 2). The specifications of these samples are listed in Tables 1 and 2.

Refrozen rounded polycrystals

The refrozen rounded polycrystals are natural and were collected from the snow observation yard of the Shinjo Branch, Snow and Ice Research Center, NIED, Japan, stored in a cold room at –20°C on 24 February 1999 and kept there for 4 months. Experiments were carried out in the cold room at –10°C on 24 and 25 June 1999. The grain size of the refrozen rounded polycrystals ranged from ~1 to 2 mm.

Small rounded particles

The small rounded particles were metamorphosed from fresh artificial snow for 1 week at –10°C. The fresh snow was grown on the rotating fins of a snow-making machine fixed to the ceiling of a 4 m high cold room (Higashiura and others, 1997). The fresh-grown snow fell onto a table in the cold room. It was then shovelled onto an approximately 0.02 m thick layer of natural, slightly wet, rounded polycrystals of snow in a 0.3 m × 0.4 m × 0.3 m cardboard box and kept in the cold room at –10°C for one night. The height of the snow block of small rounded particles was approximately 0.3 m. The grain size of the small rounded crystals ranged from ~0.2 to 0.5 mm.

Table 1. Specifications of refrozen rounded polycrystals of snow. (E^* after Mellor, 1975.) Date of experiment: 24/25 June 1999

No.	m	α	A	σ	ρ	τ	E^*	γ	Δt	$\dot{\gamma}$
	kg	10 m s^{-2}	10^{-2} m^2	10^{-1} kPa	kg m^{-3}	kPa	10^4 kPa	10^{-4}	s	10^{-3} s^{-1}
G-1	3.34	5.3	4.92	6.66	310	3.6	1.8	5.0	0.40	1.3
G-2	2.44	6.1	5.55	4.31	290	2.7	1.2	5.6	0.40	1.4
G-3	3.35	3.3	5.01	6.56	220	2.2	0.30	19	0.84	2.2
G-4	2.50	6.0	5.12	4.79	290	2.9	1.2	6.2	0.45	1.4
G-5	4.25	5.0	5.35	7.79	240	4.0	0.44	23	0.25	9.1
G-6	5.40	4.5	6.93	7.64	300	3.5	1.5	6.0	0.59	1.0
G-7	4.95	4.4	6.34	7.66	320	3.5	2.2	4.0	0.54	0.74
G-8	3.10	6.1	4.18	7.27	270	4.5	0.81	14	0.30	4.7

https://doi.org/10.3189/002214310791968502 Published online by Cambridge University Press

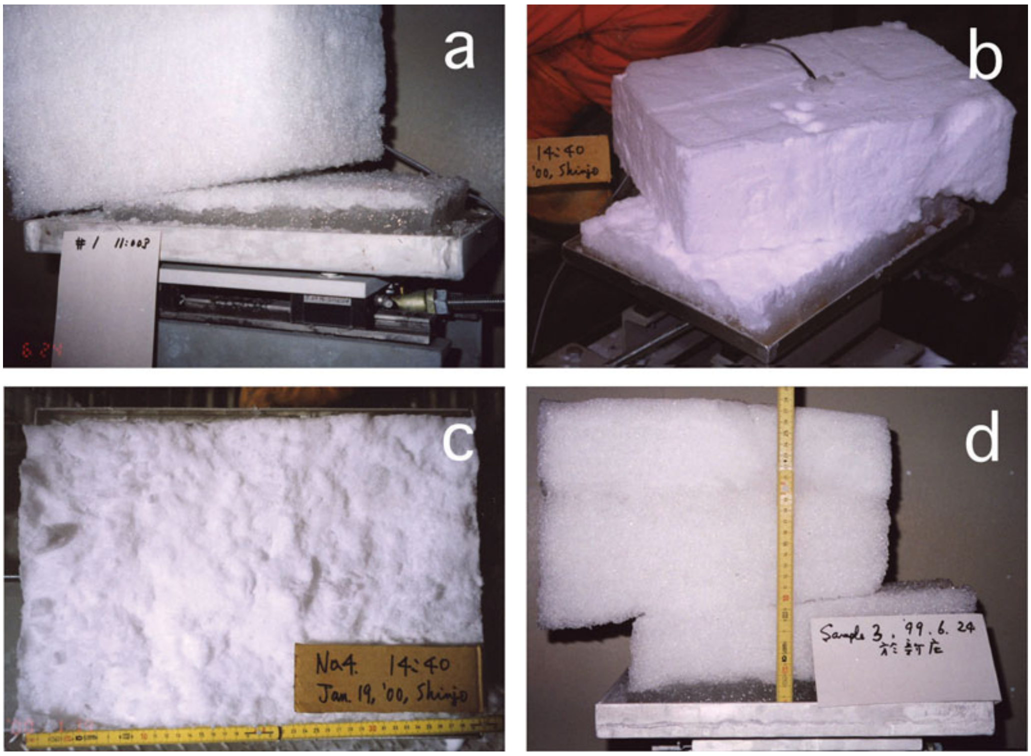

Fig. 5. Four examples of snow blocks fractured internally, where the fractured surface is planar. (a) Snow block of refrozen rounded polycrystals fractured at the base. (b) Snow block of small rounded particles fractured at the base. (c) The nearly flat plane of the snow block shown in (b), with some roughness after the snow block has been fractured. (d) Photograph showing a fracture which occurred at a weak layer in the middle of the snow block.

EXPERIMENTAL AND ANALYTICAL ASPECTS

In the cold room at –10°C, a snow sample in the form of a rectangular block was placed in an aluminium dish that was firmly fixed to the slider by screws (Fig. 2). Water at 0°C was poured into the metal dish to freeze the snow block in the dish to a height of approximately 0.01 m. From the top, an accelerometer was pushed into the snow block. After the water was completely frozen, the slider was made to vibrate, slowly at first. The rotation speed of the motor was then increased gradually until the snow block was sheared off by the applied inertial force. The accelerogram of the snow block was recorded on a paper recorder by means of the accelerometer and amplifier. An example of an accelerogram is shown in Figure 4, indicating an increase in acceleration and the maximum value at which the fracture occurred.

The maximum acceleration was measured on the accelerogram, and F was calculated using Equation (1). The sheared surface area, A, of the base of the snow block was calculated by measuring the length and width of the base of the snow block. The shear strength, τ, was then calculated using Equation (2).

Figure 5a shows an example of a snow block of refrozen rounded polycrystals fractured at the base where the fracture surface is planar. Another example of small rounded particles of snow is shown in Figure 5b, where the fractured bottom surface is planar; the roughness of the fractured

Table 2. Specifications of small rounded particles of snow. (E^* after Mellor, 1975.) Date of experiment: 19 January 2000

No.	m	α	A	σ	ρ	τ	E^*	γ	Δt	$\dot{\gamma}$
	kg	$10\,\mathrm{m\,s^{-2}}$	$10^{-1}\,\mathrm{m^2}$	10^{-1} kPa	$\mathrm{kg\,m^{-3}}$	kPa	10^3 kPa	10^{-4}	s	$10^{-3}\,\mathrm{s^{-1}}$
C-1	1.75	4.3	0.87	1.97	160	0.85	0.88	2.5	0.56	0.44
C-2	3.05	6.8	1.10	2.72	170	1.9	1.2	4.0	0.50	0.80
C-3	2.01	8.7	1.10	1.79	170	1.6	1.0	4.0	0.47	0.86
C-4	2.19	11.3	1.06	2.03	160	2.3	0.81	7.2	0.42	1.7
C-5	4.63	11.3	0.87	5.23	180	6.0	1.3	12	0.42	2.9
C-6	5.25	10.0	1.08	4.77	180	4.9	1.4	8.7	0.44	2.0
C-7	2.19	7.7	1.10	1.95	170	1.5	1.1	3.5	0.67	0.53
C-8	5.36	6.8	1.10	4.79	210	3.3	2.3	3.6	0.63	0.57
C-9	5.60	9.4	1.14	4.80	200	4.6	2.0	5.8	0.45	1.3
C-10	6.85	1.3	1.12	5.98	170	0.79	1.1	1.8	0.63	0.29
C-11	7.19	12.3	1.16	6.10	170	7.6	1.0	19	0.40	4.8

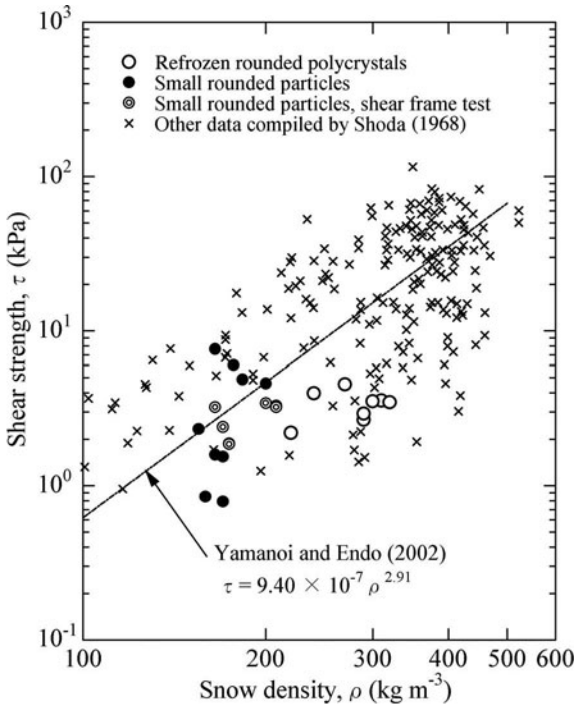

Fig. 6. Experimental data on dependence of snow shear strength on density.

bottom surface is shown in Figure 5c. When a weak layer, which is usually the boundary of the upper snow layer and lower snow layer, exists in a snow block, a fracture occurs across this layer and not at the base, as shown in Figure 5d. The fractured surface shown in Figure 5d is smoother than that shown in Figure 5c. The 0°C water that was poured into the metal dish changed into ice, as seen at the base of the snow block samples (dark areas in Fig. 5a and b). As observed in these four photographs (Fig. 5a–d), all the fractures occurred inside the snow block samples. Figure 5c shows that almost all the area is white. Therefore, it is concluded that the added water did not influence the accuracy of the measurement of the snow shear strength.

Dependence of snow shear strength on density

Data for the refrozen rounded polycrystals and small rounded particles obtained using the apparatus are plotted in Figure 6. For each of these two snow groups, there is no evidence of a shear strength dependency on snow density. The snow density range covered, however, is small, and the data do fit within the range of values found by Shoda (1968) for fine snow, rounded particles and rounded polycrystals. The equation obtained by Yamanoi and Endo (2002) for fine snow and rounded particles is also shown.

All snow blocks composed of small rounded particles fractured at their base. The rest of the snow blocks were used for a shear frame test. The shear frame tester, shown in Figure 7, has an area of 2.5×10^{-2} m^2. The results obtained with the shear frame tester are also included in Figure 6, and agree well with those from the new apparatus. Details of the data are summarized in Table 3. All shear fracture tests were carried out in a cold room at –10°C.

Table 3. Specifications of small rounded particles of snow for shear frame tests. (No. corresponds to the No. in Table 2)

No.	ρ kg m^{-3}	τ kPa
C-2	170	1.9
C-3	170	3.2
C-7	170	2.4
C-8	210	3.2
C-9	200	3.4

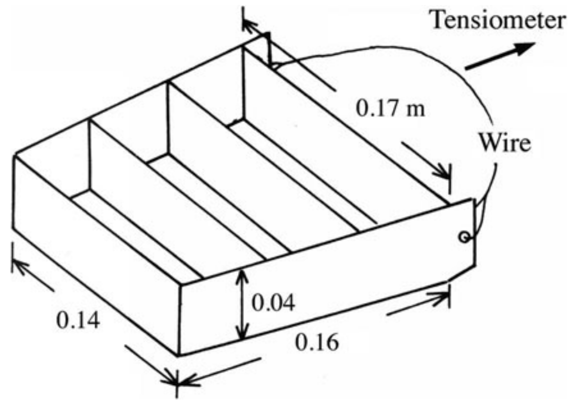

Fig. 7. Shear frame tester used for measurement.

Dependence of snow shear strength on overburden load

We applied Coulomb's equation,

$$\tau = \sigma \tan \phi + c, \qquad (3)$$

to the data. Here τ is the shear strength, σ the overburden load, ϕ the friction angle and c the cohesion. After every experimental run, the mass of the fractured snow block was weighed and the overburden pressure, σ (kPa), was calculated. Bricks were placed on the snow block to increase the overburden weight. Figure 8 shows the dependence of snow shear strength on overburden load. From the data, a linear regression curve was obtained for the refrozen rounded

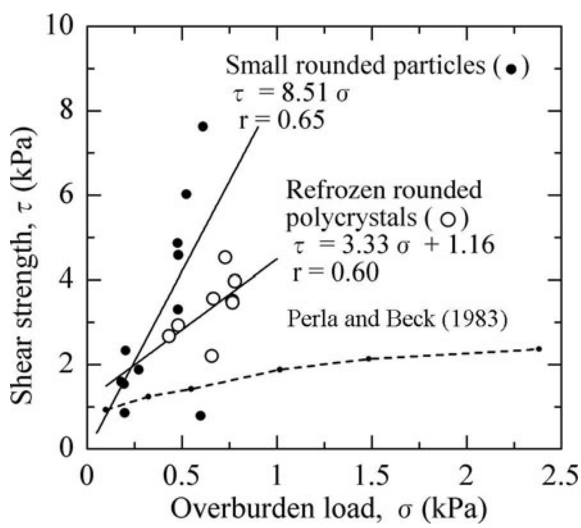

Fig. 8. Experimental data on dependence of snow shear strength on overburden load.

https://doi.org/10.3189/002214310791968502 Published online by Cambridge University Press

polycrystals:

$$\tau = 3.33\sigma + 1.16\ (r = 0.60)\ \text{(kPa)}. \quad (4)$$

For small rounded particles,

$$\tau = 8.51\sigma\ (r = 0.65)\ \text{(kPa)}. \quad (5)$$

For small rounded particles, the constant cohesion term is neglected because its value is small, –0.05.

In Figure 8, we also include a shear strength curve obtained by Perla and Beck (1983), which shows normal load dependence measured on a layer of partially metamorphosed crystals ($\rho = 200\,\text{kg m}^{-3}$). This curve shows a gradual but nonlinear shear strength increase with overburden load.

Dependence of snow shear strength on strain rate

In the case of an elastic body, the shear modulus, G, shear stress, τ, shear strain, γ, Young's modulus, E, and Poisson ratio, ν, are related by

$$G = \tau\gamma^{-1} = 1/2E(1+\nu)^{-1}. \quad (6)$$

Thus we obtain

$$\gamma = 2\tau(1+\nu)E^{-1}. \quad (7)$$

We do not measure the values of E and ν for the snow blocks. Rather, we read the average values from a figure provided by Male (1980; after Mellor, 1975) for the snow density dependence of E. For ν, the average value (0.264) of tension and compression data obtained by Shinojima (1993) was used. The strain rate, $\dot{\gamma}$, is calculated as $\dot{\gamma} = \Delta\gamma/\Delta t$. Δt is the time taken to reach the peak value of the vibration curve when the fracture occurs, as shown in Figure 1.

Figure 9 shows the shear strength of snow as a function of shear strain rate. There seems to be a trend to increasing shear strength with strain rate for small rounded particles. In the case of the refrozen rounded polycrystals, there also seems to be a trend but it is not as strong. Data obtained by Schweizer (1998), which seem to indicate a counter-trend (i.e. decreasing shear strength with increasing shear strain rate), are also presented.

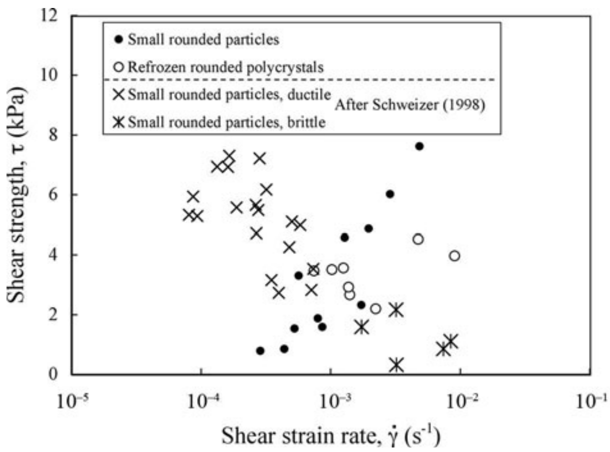

Fig. 9. Experimental data on dependence of snow shear strength on strain rate.

DISCUSSION AND CONCLUSIONS

The principle underlying the fabricated apparatus is simple and appears to work well. The apparatus is inexpensive, simple to use and works smoothly with good repeatability, although it is not portable.

We found a dependence of snow shear strength on density, but the trend is not statistically significant over the small range of densities studied. More data over a larger density range are clearly needed. Our values did fall within the range of those found by Shoda (1968) and agree well with data obtained using a shear frame tester.

We found a linear dependence of snow shear strength on overburden load. For small rounded particles, the dependence is stronger ($\tau/\sigma = 8.51$) than for refrozen rounded polycrystals ($\tau/\sigma = 3.33$). Also, for small rounded particles, the constant cohesion term (Coulomb's equation) was found to be near zero. The dependence we found, of snow shear strength on overburden load, was also stronger than that found by Perla and Beck (1983). At higher densities than we studied (239, 351 and $402\,\text{kg m}^{-3}$) in the overburden load range, 0–12 kPa, Yamanoi and Endo (2002) noticed no significant shear strength dependence on normal load for snow consisting of small rounded particles. However, at values (average density of four data $168\,\text{kg m}^{-3}$; overburden load range 0–3 kPa) similar to those we studied, they observed a shear strength dependence on normal load in half of them. The other half showed no significant dependence.

For low-density snow ($300\,\text{kg m}^{-3}$) in tension, Narita (1980, 1983) found a peak in the maximum shear strength as a function of shear strain rate. The peak occurred at a strain rate of $10^{-4}\,\text{s}^{-1}$. For strain rates below $10^{-4}\,\text{s}^{-1}$, the maximum tensile strength increases with increasing strain rate (plastic or ductile deformation); for strain rates above $10^{-4}\,\text{s}^{-1}$, the maximum tensile strength decreases with increasing strain rate (brittle deformation). Schweizer's (1998) data clearly demonstrate brittle deformation in the strain-rate range $\sim 10^{-4}$–$10^{-2}\,\text{s}^{-1}$ (Fig. 9). While our data were obtained in the same strain-rate range, they show the opposite trend, i.e. increasing shear strength with increasing strain rate. Other factors (e.g. temperature, frequency specification of the apparatus) may account for this discrepancy, and further studies are clearly required.

In summary, our apparatus and our analytical method can be used efficiently to measure the shear strength of snow. However, the effects of the vibration cycles before fracture have not been elucidated. The shear strength of snow measured using our new apparatus might be called dynamic shear strength, and that measured using a frame tester, static shear strength. In future, discussion of the difference between these two measures might lead to new studies of the shear strength of snow. We believe that further study is required to elucidate the dependence of shear strength on density, overburden load and strain rate. We hope this new apparatus will aid these future studies.

ACKNOWLEDGEMENTS

We thank J. Glen for critical reading and advice on an earlier draft of this paper and for scientific edting of the final version. We thank M. Irasawa, K. Kakuta, and Y. Kubodera for creating some initial figures. We thank V. Aizen for showing interest in the paper; this eventually helped us to obtain the final title. We thank T.H. Jacka, E. Morris and an anonymous reviewer for critical reading and comments that improved the paper. We also thank K. Shinojima for reading the initial manuscript.

REFERENCES

Abe, O. 2004. Shear strength and angle of repose of snow layers including graupel. *Ann. Glaciol.*, **38**, 305–308.

Abe, O. *and 7 others*. 2006. Shear strength of natural and artificial depth hoar layers. *In* Gleason, J.A., *ed. Proceedings of the International Snow Science Workshop, 1–6 October 2006, Telluride, Colorado*. Telluride, CO, International Snow Science Workshop, 7–14.

Colbeck, S.C. *and 7 others*. 1990. *The international classification for seasonal snow on the ground*. Wallingford, Oxon, International Association of Hydrological Sciences. International Commission on Snow and Ice.

Föhn, P.M.B. 1987. The stability index and various triggering mechanisms. *IAHS Publ.* 162 (Symposium at Davos 1986 – *Avalanche Formation, Movement and Effects*), 195–214.

Gürer, I. 1993. Snow avalanche disaster of winter 1992 in southeastern Anatolia, Turkey. *Seppyo, J. Jpn. Soc. Snow Ice*, **55**(1), 41–48.

Higashiura, M., T. Nakamura, H. Nakamura and O. Abe. 1979. An avalanche caused by an earthquake. *Rep. Nat. Res. Cent. Disaster Prevent.* 21, 103–112. [In Japanese with English summary.]

Higashiura, M. *and 6 others*. 1997. Preparation of the experimental building for snow and ice disaster prevention. *In* Izumi, M., T. Nakamura and R.L. Sack, *eds. Snow engineering: recent advances*. Rotterdam, A.A. Balkema, 605–608.

Jamieson, B. and C.D. Johnston. 2001. Evaluation of the shear frame test for weak snowpack layers. *Ann. Glaciol.*, **32**, 59–69.

Male, D.H. 1980. The seasonal snowcover. *In* Colbeck, S.C., *ed. Dynamics of snow and ice masses*. New York, Academic Press, 305–395.

McClung, D.M. 1977. Direct simple shear tests on snow and their relation to slab avalanche formation. *J. Glaciol.*, **19**(81), 101–109.

Mellor, M. 1975. A review of basic snow mechanics. *IAHS Publ.* 114 (Symposium at Grindelwald 1974 – *Snow Mechanics*), 251–291.

Nakamura, T., O. Abe and S. Takada. 1992. Roof snow observation and the application to the house construction. *CRREL Spec. Rep.* 92-27, 81–92.

Nakamura, T., Y. Nohguchi, T. Kobayashi, Y. Yamada, K. Ohtani and S. Takada. 1997. The reduction of earthquake energies on buildings by snow on their roofs. *In* Izumi, M., T. Nakamura and R.L. Sack, *eds. Snow engineering: recent advances*. Rotterdam, A.A. Balkema, 193–200.

Nakamura, T., O. Abe, Y. Nohguchi and T. Kobayashi. 2000. *[Fundamental study of the reduction in disasters due to the combined effect of heavy snowcover on the roof and earthquakes.]* Tokyo, Secom Science and Technology Foundation, 66–70. (Collected Report 19.) [In Japanese.]

Narita, H. 1980. Mechanical behaviour and structure of snow under uniaxial tensile stress. *J. Glaciol.*, **26**(94), 275–282.

Narita, H. 1983. An experimental study on tensile fracture of snow. *Contrib. Inst. Low Temp. Sci., Ser. A* 32, 1–37.

Perla, R. and T.M.H. Beck. 1983. Experience with shear frames. *J. Glaciol.*, **29**(103), 485–491.

Perla, R., T.M.H. Beck and T.T. Cheng. 1982. The shear strength index of alpine snow. *Cold Reg. Sci. Technol.*, **6**(1), 11–20.

Schweizer, J. 1998. Laboratory experiments on shear failure of snow. *Ann. Glaciol.*, **26**, 97–102.

Shinojima, K. 1993. Experimental study on the mechanical property of snow. (PhD thesis, Nagaoka University of Technology.)

Shoda, M. 1968. [Mechanical property of snow]. *In [Handbook for mitigation and prevention of snow disasters]*. Tokyo, Japan Construction Mechanization Association, section 1.2. [In Japanese.]

Watanabe, Z. 1977. The influence of snow quality on the breaking strength. *Sci. Rep. Fukushima Univ.* 27, 27–35.

Yamanoi, K. and Y. Endo. 2002. Dependence of shear strength of snow cover on density and water content. *Seppyo, J. Jpn. Soc. Snow Ice,* 64(4), 443–451. [In Japanese with English summary.]

MS received 29 May 2009 and accepted in revised form 27 March 2010